We are IntechOpen,
the world's leading publisher of
Open Access books
Built by scientists, for scientists

6,900
Open access books available

186,000
International authors and editors

200M
Downloads

Our authors are among the

154
Countries delivered to

TOP 1%
most cited scientists

12.2%
Contributors from top 500 universities

WEB OF SCIENCE™

Selection of our books indexed in the Book Citation Index
in Web of Science™ Core Collection (BKCI)

Interested in publishing with us?
Contact book.department@intechopen.com

Numbers displayed above are based on latest data collected.
For more information visit www.intechopen.com

Dynamic Characteristics of Linear and Nonlinear Wideband Photonic Crystal Filters

I. V. Guryev, J. R. Cabrera Esteves, I. A. Sukhoivanov,
N. S. Gurieva, J. A. Andrade Lucio,
O. Ibarra-Manzano and E. Vargas Rodriguez

Additional information is available at the end of the chapter

1. Introduction

In the chapter, we give results of investigation of dynamics of linear and nonlinear photonic crystals (PhC).

It is well-known fact that modern semiconductor electronic data processing systems are experiencing fundamental problems with further improvement of the microprocessors productivity. One of the alternative ways is to use hybrid or all-optical circuits on the basis of PhCs.

The heart of such all-optical circuit is nonlinear PhC which may provide the basis for logic, memory cells, switching, local routing, power limiters, isolators, etc. Therefore, it is of crucial importance to understand the processes taking place in such components and optimize their characteristics. One of the most important points of view to the PhCs is their interaction with short and ultra-short pulses which may limit the productivity of an optical circuit. Recently, there have been proposed a great number of PhC components bases on different operating principles. However, being resonant-transmitting structures, PhCs themselves reduce the possibility to work with ultra-short pulses.

In the papers of the authors, it have been proposed to use wideband PhC filters instead of high-Q ones [9], [6]. Lower resonant properties as compared to high-Q filters, allow to reduce distortion of the signal passing through such filters. In this chapter we present the investigation results and analysis of the temporal response of different kinds of wideband PhC filters. Namely, we consider filters made of linear optical materials which can be used for local multiplexing and routing and the ones made of nonlinear optical materials which properties strictly depend on the radiation intensity.

We explain the computation process of such characteristics of the PhC filters as transmission spectra, eye-diagrams and the band structure.

The chapter is organized as follows:

In the first section of the chapter, we briefly explain theoretical background under the computation of dynamic characteristics of micro-devices. Then, in the second section, we give the results of investigation of linear wideband PhC filters. We concentrate attention on transmission spectra and an eye-diagram of such filters. Finally, we demonstrate application of the PhC filters to the wavelength division multiplexing and analyze their limitations. The third section of the chapter is dedicated to nonlinear PhC filters and their characterization. We first present one of the methods of the band structure computation of nonlinar PhCs. After this, we investigate such important application of the nonlinear PhC filters as all-optical flip-flop which may become the basis of optical data processing systems.

Although we do not provide here the detailed description of the physical processes below the presented characteristics, the reader can find them in the book "Photonic Crystals: Physics and practical modeling" [8]

2. Computing the temporal response of the PhC filter

The term PhC is usually used to define infinite periodic structure. However, such structures do not have many practical applications since they only possess artificial reflecting and refracting properties and cannot control effectively the radiation flow. To implement effective radiation flow control, we have to create at least one defect of the periodic structure to be able to localize the radiation. However, in real devices, we should be able to provide light guiding, localization and dynamic routing.

Therefore, speaking of PhC devices we are usually assume their complex structure which cannot be represented by strictly periodic variation of the refractive index. In this situation, the only way to find the field distribution inside the PhC device is to apply numerical methods. Due to recent advance in computing technologies, there have been appeared a wide variety of numerical methods giving time-dependent field distribution in complex nonlinear media. Most of them are highly time- and resource-consumable. However, the most easy to implement and, yet, quite effective is the finite difference time-domain (FDTD) method which allows computing field distribution in nonlinear complex media such as PhC devices.

In general, there have to be considered complete system of Maxwell's equations which, in linear case represents six (or even twelve [1]) equations. One simplification can be made though. Namely, most of the models are based on 2D PhC of different configuration since they possess wide photonic band gap and, on the other hand, provide enough flexibility to design wide variety of the components.

The system of Maxwell's equations can be reduced to 2D case considering certain polarization. Namely, in case of TM polarization (as referred to in [7]), we have the following system of equations [11]:

$$\frac{\partial}{\partial t} H_x = -\frac{1}{\mu_0} \frac{\partial}{\partial y} E_z,$$

$$\frac{\partial}{\partial t} H_y = \frac{1}{\mu_0} \frac{\partial}{\partial x} E_z, \tag{1}$$

$$\frac{\partial}{\partial t} E_z = \frac{1}{\varepsilon_0} \left(\frac{\partial}{\partial x} H_y - \frac{\partial}{\partial y} H_x - J_z \right),$$

and in case of TE polarization:

$$\frac{\partial}{\partial t} E_x = \frac{1}{\varepsilon_0} \left(\frac{\partial}{\partial y} H_z - J_x \right),$$

$$\frac{\partial}{\partial t} E_y = \frac{1}{\varepsilon_0} \left(-\frac{\partial}{\partial x} H_z - J_y, \right) \tag{2}$$

$$-\frac{\partial}{\partial t} H_z = \frac{1}{\mu_0} \left(\frac{\partial}{\partial x} E_y - \frac{\partial}{\partial y} E_x \right),$$

where $\vec{J}$ is an electric current density which, properly defined, determines nonlinearity of the material.

Particularly, in case of non-saturable Kerr nonlinearity polarization current density is given in following form [4]:

$$\vec{J} = \frac{\partial \vec{P}}{\partial t} = \frac{\partial}{\partial t} \varepsilon_0 \chi^{(1)} \vec{E} + \frac{\partial}{\partial t} \varepsilon_0 \chi^{(3)} |\vec{E}|^2 \vec{E} \tag{3}$$

where $\chi^{(1)}$ and $\chi^{(3)}$ are the terms of linear and nonlinear susceptibility.

However, materials usually possess non-saturable Kerr properties only within low radiation intensity range and, therefore, we consider Kerr-saturable nonlinear materials and nonlinear susceptibility terms. Assuming slowly varying amplitude of the field $\left(\frac{\partial}{\partial t} |\vec{E}|^2 \approx 0 \right)$, we can present nonlinear polarization term, by the analogy with [2], in following form:

$$\vec{P} = \varepsilon_0 \chi_0^{(3)} \frac{|\vec{E}|^2}{1 + |\vec{E}|^2 / I_{sat}} \vec{E}, \tag{4}$$

and corresponding polarization current takes form:

$$\vec{J} = \frac{\partial}{\partial t} \varepsilon_0 \chi^{(1)} \vec{E} + \frac{\partial}{\partial t} \varepsilon_0 \chi_0^{(3)} \frac{|\vec{E}|^2}{1 + |\vec{E}|^2 / I_{sat}} \vec{E} \tag{5}$$

where nonlinearity term is now presented in form of saturable function.

Applying the FDTD technique expanded with auxiliary differential equation for the nonlinear medium [4] with polarization current given in form of (5) and assuming perfectly-matched layer [1] at the boundary of computation region, we can compute time-dependent electromagnetic field distribution in nonlinear saturable media.

3. Passive wideband PhC filters

Modern trends in data processing and transmission systems require new compact and high-speed solutions for all-optical circuits. Particularly, this concerns precise spectral filtering which can be implemented on the basis of PhCs. Recently, two wide categories of the PhC filters have been investigated, namely, high-Q and wideband ones. The first kind of filters possesses incredible spectral characteristics and suppose to be used in telecommunication for dense WDM demultiplexing. However, such filters have several disadvantages which make them hardly implemented in the nearest future. Particularly, recently designed high-Q filters require technology precision which is only possible in laboratory conditions. Moreover, due to their resonant nature, such filters cannot be used in the systems utilizing ultra-short pulses.

On the other hand, wideband filters which Q-factor is much lower than the one of the high-Q filter, possess comparatively low resonant properties which makes them suitable for ultra-short pulses application. Moreover, their characteristics are not affected too much by slight variation of the geometric parameters.

3.1. PhC filters spectrum

When designing wideband PhC filters, first thing we need to know is their spectral properties. Various numerical methods can be applied to compute such characteristics.

Particularly, when using the FDTD method, there are two different ways to find transmission or reflection spectrum of the PhC device. The first one is based on analysis of the response to continuous wave (CW) radiation. The second method uses Fourier analysis of the pulsed signal.

Analysis of the pulsed response is fast and accurate way to compute the spectrum. Basically, it is computed as a Fourier transform of the temporal response of the structure taken in certain spatial point.

However, this technique is only suitable when dealing with transversally-confined radiation (i.e. in case of the PhC waveguides as shown in Figure 1a). When it is necessary to find the spectrum in case of scattered radiation distribution (as presented if Figure 1b), the spectrum should be computed for each spatial point of interest.

3.1.1. Analysis of the CW response of the structure

CW signal usually possesses very narrow spectra and, therefore, computing the structure response to the CW we find its transmission of reflection at a specific wavelength. To compute the whole spectrum of the structure the response should be obtained at several wavelengths according to required spectrum.

To provide high accuracy of the method, several criteria should be satisfied:
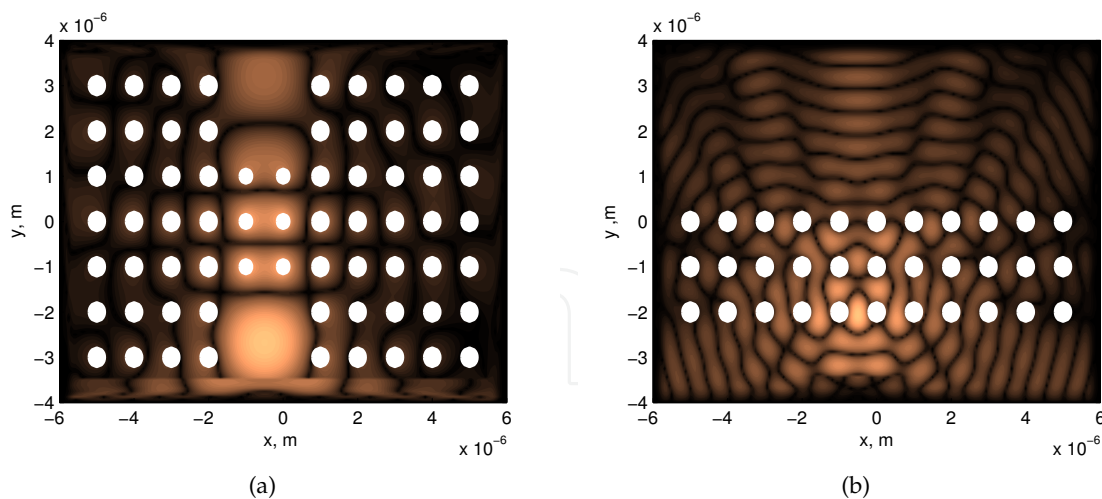
Figure 1. Confined or concentrated (a) and scattered (b) field distribution

- Every moment of time the radiation should be integrated along all the area of interest.
- Computation time should be long enough to achieve constant radiation intensity at the output (i.e. to pass all the transition processes).
- Spectral points should be selected close enough to avoid discontinuities of the final spectrum.

In case of PhC devices, the main application of such technique is computing the transmission spectra of bulk PhCs where the radiation is scattered.

3.1.2. Analysis of the pulse response of the structure

Unlike the CW radiation, pulsed one possesses wide spectrum which can be easily found from its Fourier transform.

To find the transmission spectrum of the PhC filter, it is first necessary to find temporal response of the filter to the launched Gaussian pulse (or any other wide-spectrum pulse). The temporal response is taken at a single spatial point. After a certain time, the Fourier transform of the temporal response can be taken. However, the spectrum obtained in such a way depends on the spectrum of the pulse launched to the system. Therefore, to find the final spectrum of the structure it is necessary to divide it by the spectrum of the initial pulse.

In general, to implement the method, certain steps should be made:

1. Set up the structure (i.e. define the refractive index distribution)
2. Set up the launch field before the structure
3. Run the simulation for a time much longer than the pulse lasts. The longer the simulation lasts, the higher the resolution of the spectrum will be.
4. Save the temporal distribution of one the field components after the structure
5. Find the Fourier transform of this temporal distribution.
6. Normalize the frequency.

3.2. Building an eye-diagram

In the electronic devices design and testing, it is usually used an eye-diagram to determine the quality of the transition characteristics. In fact, an eye diagram is represented by the series of the device work cycles drawn one over another. During this cycles the device is randomly turned on and off. Resulting characteristic resembles a human eye. If an "eye" is "closed" this points to poor quality of the device. In its "open" state, an eye's dimensions define parameters of the device such as bit error rate (BER).

In case of active and passive PhC wideband filters, an eye diagram can be used as well to define the quality of the device. Since a PhC possesses resonant transmission (i.e. the radiation is propagated from one element to another) after the device working cycle a fraction of an optical radiation is still remaining in the PhC elements. If this fraction is large enough, it will interfere with the next pulse resulting in radiation accumulation from pulse to pulse. After several pulses, the remaining radiation level can be large enough to affect the functioning of the nonlinear device or produce an error bit.

To detect such effects and also to find the pulse shape variation at the output of the PhC filter, an eye-diagram of the device can be built and analyzed.

Let us consider the process of building an eye-diagram of a simple nonlinear PhC wideband filter working at the edge of the photonic band gap. The filter is confined with linear PhC waveguide. We will now investigate its response to the sequence of Gaussian signals of different periods. In the first case, the period is large enough to release the radiation completely. The second pulses series possesses higher frequency.

The response of the filter in both cases is given in top of the Figure 2. To build an eye-diagram, it is important to know the period of the pulses (which in most cases is not obvious from the response). Since we know the repetition rate of the input pulses, we will use it. Now we only need to skip the transition time of the filter and split the response characteristic into equal pieces. Here we present the Matlab program which builds an eye-diagram from the response to the random pulses series. The response should be saved into a separate file in form of sequence "Time   E(Time)".

```
%The program is intended to represent computed
%temporal response of an optical structure to
% a series of pulses, as an eye–diagram. The
%response should be given in form of amplitute–vs–
%time

%Number of pulses in the response
num_pulses=30;
%Number of time–points within one pulse
%It should be determined from a computation method
period=1280;
%Initial point of the series (non–zero due to
%finite value of the speed of light)
t0=period;
```

%Loading the data with stored temporal response
data=load('`response.dat`');

%Creating a figure
figure;
subplot(2,1,1);
%Plotting the response
plot(data(:,1), data(:,2));
ylabel('`|E|^2`');

ax=subplot(2,1,2);

hold on;
%The data for the X−axis (time within the period)
time=data(1:period+1,1);
%Plotting every period in the same figure
for i=0:num_pulses−1
    plot(time, data(t0+(i∗period:(i+1)∗period),2), '`o`')
end
set(ax, '`XGrid`','`on`');
set(ax, '`YGrid`','`on`');
xlabel('`Time, s`');
ylabel('`|E|^2`');
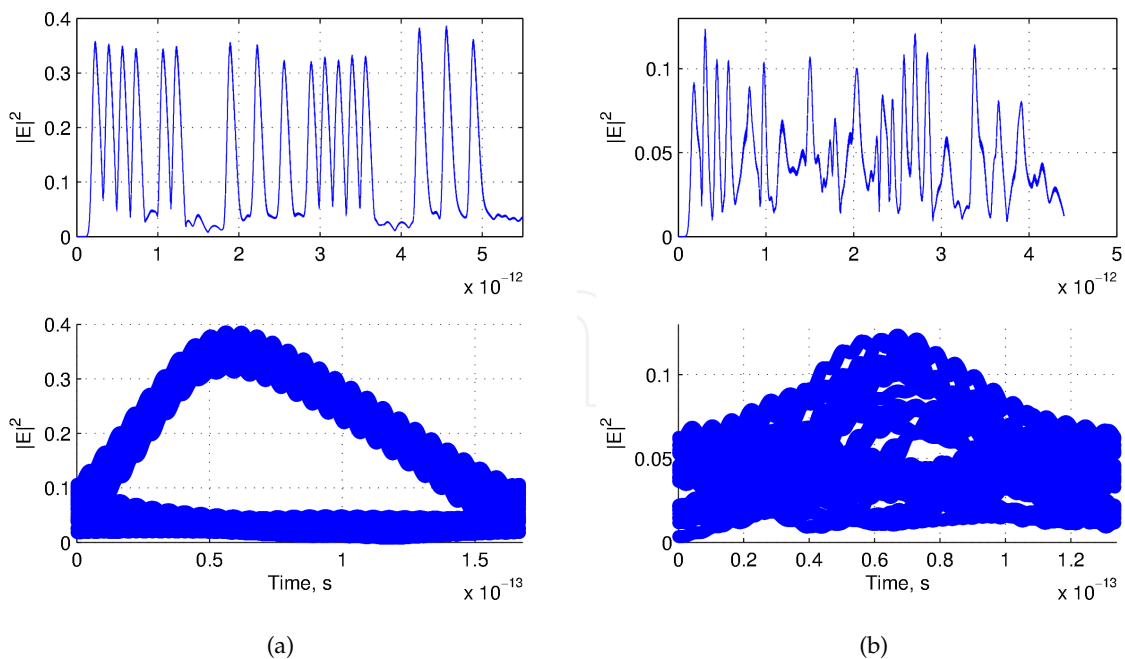
Figure 2. Examples of generated eye-diagrams. a) With weak pulse perturbation and b) with strong pulse perturbation

In the bottom parts of the Figure 2 we give two cases of an eye-diagram computed for a single PhC filter at different pulse duration. In the first case, an "eye" is clearly opened which tells us that the radiation is not accumulated in the filter. On the other hand, when pulse repetition rate is too high, the radiation is accumulated within the PhC which is reflected in the diagram (an "eye" is closed in Figure 2b). Investigating the shape of the pulse, we can also make a conclusion about how much does filter distort the pulse shape. For instance, even in the Figure 2a, the output pulse shape is obviously non-Gaussian due to distortions introduced by the filter.

3.3. PhC wavelength division demultiplexer

One of the most basic and, on the other hand, important applications of a passive PhC is a wavelength division demultiplexer. In multi-wavelength systems it provides spatial separation of the wavelength-mixed signal.

One of possible structures providing two-channel demultiplexing is presented in the Figure 3a. A signal containing two wavelengths enters through the bottom part of the device, travels to the coupler where it is separated by the wideband filters.

(a)   (b)
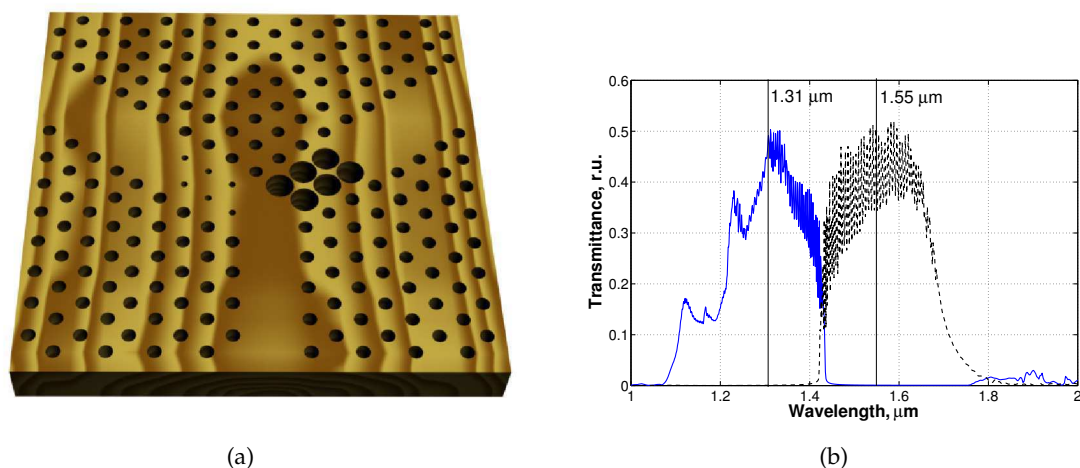
Figure 3. Structure of the PhC demultiplexer (a) and the spectra of the output channels (b)

Resulting spectra found by analyzing temporal response of the filters is presented in Figure 3b.

However, knowing spectral properties is not enough to characterize the demultiplexer completely. Since each PhC device possesses resonant properties, it is necessary to investigate distortions introduced to the signal when passing this device. This can be done by computing an eye-diagram of each wavelength channel (see Figure 4). Here we presented the diagrams computed for the pulses sequence with period $T = 160\ fs$ and pulse width of about $\tau = 80\ fs$

Presented eye-diagrams demonstrate that the demultiplexer can be used to process the ultra-short pulses. However, in case of $\lambda = 1.55\ \mu m$ the filter introduces more distortion into a pulse shape (i.e. pulse shape is not Gaussian at the output of the filter). This fact does not affect too much if a single device is used. However, when implementing an integrated optical circuit including series of linear and nonlinear filters, such distortions should be minimized to prevent data losses in the circuit.
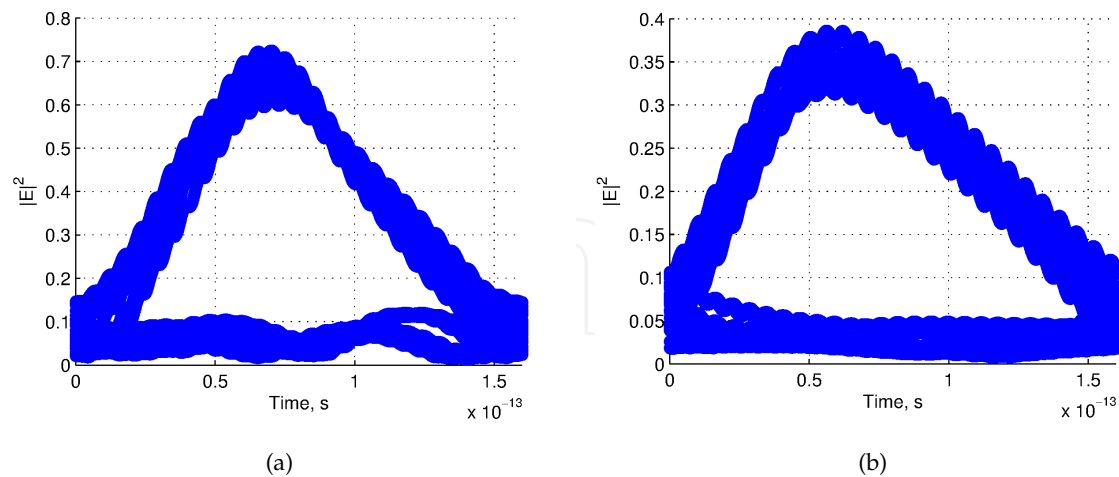
Figure 4. Eye diagrams of the PhC demultiplexer at 1.31 μm (a) and 1.55 μm (b)

4. Temporal characteristics of active PhC filters

4.1. Nonlinear PhC band structure

The band structure of the PhC can be computed by means of different methods. Among them, the most fast is the plane wave expansion (PWE) method. However, PWE has drawbacks which do not allow it to be applied to active PhCs. Namely, it is impossible to take into consideration the chromatic dispersion, absorption and gain as well as nonlinear material properties when refractive index depends on the radiation intensity.

One of possible ways to overcome the problem is to apply the FDTD technique. In contrast to the PWE method, the FDTD allows to take into account the refractive index variation during the computation process [11] and, therefore, to compute the light propagation in the nonlinear materials.

Here, we consider basic principles underlying the band structure computation by means of FDTD technique which are briefly discussed, for example, in [12].

In general, PBG computation using FDTD should be carried out as follows:

1. Determine the computation area.

2. Set up periodic boundary conditions.

3. Define the radiation excitation function. The radiation spectrum should be wide enough to cover whole investigated frequency range.

4. Carry out the spectral analysis of the time-dependent response of the structure on the probe pulse by searching all of local maxima and plotting them over frequency axis.

5. Repeat steps from 2 to 4 at different values of the phase shift in periodic boundary conditions corresponding to all selected points within the PhC Brillouin zone the band structure is computed for.
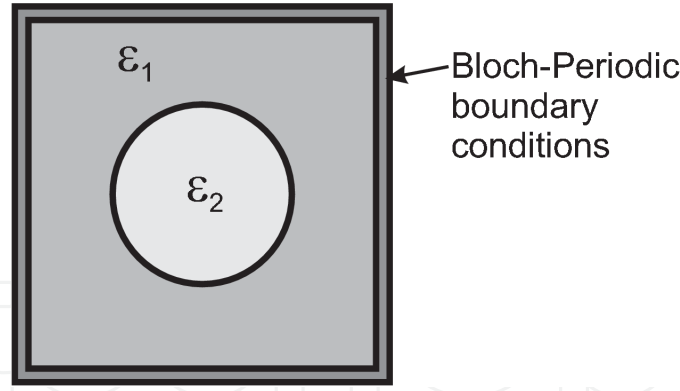
Figure 5. Computation domain for 2D PhC with square lattice

Let us now consider in details each step.

To perform any FDTD simulation, it is first necessary to determine the computation domain. However, since the PhC is considered as an infinite structure and computation over an infinite structure takes infinite time, the response of such a structure is impossible to find. Solution in this case is considering a single unit cell since it carries the information about whole structure. The computation domain in case of 2D PhC with square lattice is presented in figure 5.

The periodicity of the structure is achieved by setting up periodic boundary conditions at the edges of the computation domain.

Besides the translation emulation the periodic boundary conditions should provide simulation of electro-magnetic field propagation with certain wave vectors. Such kind of periodic boundary conditions are referred to as Bloch periodic boundary conditions [10]. The expressions of Bloch's periodic boundary conditions for electric and magnetic field components take following form:

$$
\begin{aligned}
\vec{E}\left(x+a,y+b,z+c\right) &= \vec{E}\left(x,y,z\right) \cdot e^{-\vec{i} \cdot k_x \cdot a - \vec{j} \cdot k_y \cdot b - \vec{k} \cdot k_z \cdot c}, \\
\vec{H}\left(x+a,y+b,z+c\right) &= \vec{H}\left(x,y,z\right) \cdot e^{\vec{i} \cdot k_x \cdot a + \vec{j} \cdot k_y \cdot b + \vec{k} \cdot k_z \cdot c}.
\end{aligned}
\tag{6}
$$

where a, b, c are linear dimensions of the unit cell along X, Y and Z axes respectively; k_x, k_y, k_z are wave vector components.

When applying simple periodic boundary conditions, the electric or magnetic field intensity is taken from one boundary of the computation region and is added to the corresponding field component at the opposite boundary. However, in contrast to simple periodic conditions, the Bloch ones include phase shift achieved by multiplying the field intensity by the exponential function which argument contains radiation wave vector.

Therefore, setting up the Bloch periodic boundary conditions provides the possibility to investigate propagation of radiation possessing different wave vectors to compute the band structure.

The next important moment is an input signal parameters.
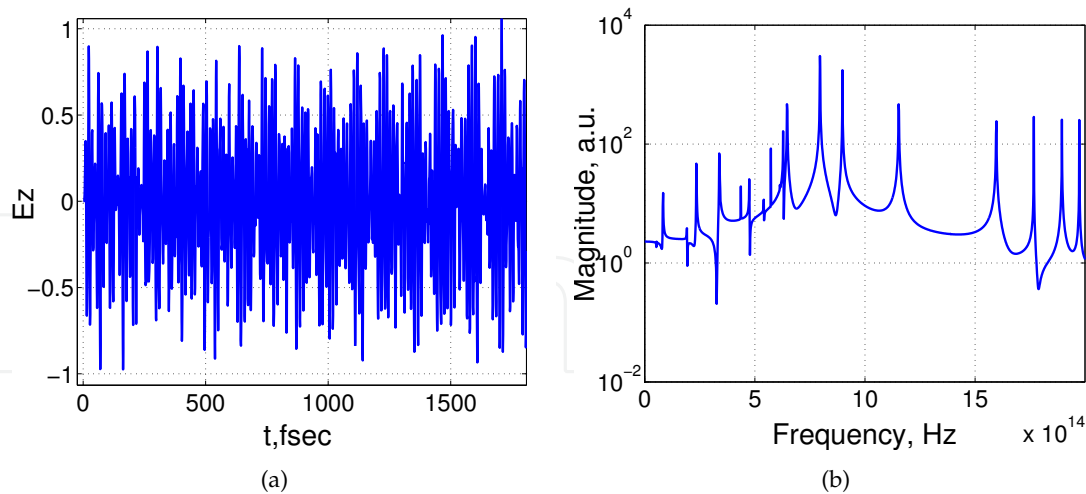
Figure 6. Temporal response (a) and its spectrum obtained by FFT (b)

The radiation can be introduced to the structure in various ways. However, we will consider excitation from a single point of the computation region. Since we are going to search for the resonant frequencies of the PhC within wide spectrum range, an input pulse should possess wide spectrum. The simplest signals used in this case are delta-pulse and Gaussian pulse. The delta-pulse in introduced in a single moment of time while the modulated Gaussian signal should be excited continuously during all simulation. It is obvious that using delta-pulse is the most simple case which we will use in our example:

$$\delta \left(t - t_0, x - x_0, y - y_0, z - z_0 \right) = 1. \tag{7}$$

It is widely known that the spectrum of the delta-pulse is infinitely wide so it gives structure responses at any frequency. After the delta-pulse is introduced, the excitation is turned off, however, due to periodic boundary conditions, radiation exists infinitely long time in the structure without absorption.

After the pulse response of the structure is obtained, it should be properly analyzed. This analysis gives eigen-states of the PhC.

The spectral analysis of the time dependent pulse response can be carried out by Fourier transform. The accuracy of the method achieves its maximum when computation time is infinite. However, since we have finite computer resources, the computation time is taken long enough just to prevent spurious solutions.

Fast Fourier transform (FFT) [3] is usually used within this technique since the response function is discrete one and in this case the FFT performance is much faster then general Fourier transform. As a result of the FFT, we have the discrete spectrum as well. The example of the FFT of the structure response to the delta-pulse excitation is shown in figure 6

The eigen-states of the structure are searched for as local maxima at the response spectrum. Detailed analysis should be made to avoid spurious solutions. Such spurious solutions are

usually appear as inessential peaks at the spectrum. Therefore, the local maximum does not always correspond to the eigen-state. The maxima corresponding to spurious solutions are just a little bit higher than neighbor spectrum points while valid solutions values give peaks with magnitudes several times larger than the one of neighbor points.

Here, we present the Matlab program for computation of the band structure of 2D PhC with square lattice. For simplicity, we consider a PhC made of linear material. To obtain the band structure of a nonlinear PhC, an auxiliary differential equation technique should be added in the FDTD part.

```
%The program is intended to compute
%the band structure of 2D PhC by means of
%the FDTD method.

%Cleaning up previous workspace
clear all;

%Setting up parameters of the PhC
%PhC period in each direction
maxX=1e−6;
maxY=1e−6;
%Radius of the cilinder
r=maxX∗0.3;
%Refractive index of the cilinder
eps1=9;
%Background refractive index
eps2=1;
%Permeability (is always 1 for non−magnetic materials)
mu=1;

%Speed of light
c=3e8;

%Setting up FDTD parameters
%Computation time
maxT=2^13;

%Number of spatial points in the grid in each direction
accuracyX=16;
accuracyY=16;
%Number of k−points between high−symmetry points
accuracyK=5;

%Defining statial and temporal steps
Dx=maxX/accuracyX;
Dy=maxY/accuracyY;
Dt=Dx/2/c;
```

```
%Defining the unit cell permittivity distribution
%Central coordinates
x0=maxX/2;
y0=maxY/2;

%For smooth permittivity profile, defining the width of
%transition zone
dd=sqrt(Dx^2+Dy^2);
%Correcting the radius according to transition zone
r=r−dd/2;
%Generating the permittivity profile
eps=ones(accuracyX, accuracyY)∗eps2;
for i=1:accuracyX
    for j=1:accuracyY
        if sqrt((i∗Dx−x0)^2+(j∗Dy−y0)^2)<r
            eps(i,j)=eps1;
        elseif sqrt((i∗Dx−x0)^2+(j∗Dy−y0)^2)−r<dd
            if(eps1>eps2)
                eps(i,j)=eps1−abs(eps1−eps2)/dd∗(sqrt((i∗Dx−x0)^2+...
                    (j∗Dy−y0)^2)−r);
            else
                eps(i,j)=eps1+abs(eps1−eps2)/dd∗(sqrt((i∗Dx−x0)^2+...
                    (j∗Dy−y0)^2)−r);
            end

        end

    end
end

%For faster FDTD computation we find the coefficients
%in the FD equations
eps_x=c∗Dt/Dx./eps;
eps_y=c∗Dt/Dy./eps;

%Defining k−path
kx(1:accuracyK+1)=0:pi/maxX/accuracyK:pi/maxX;
ky(1:accuracyK+1)=zeros(1,accuracyK+1);

kx(accuracyK+2:accuracyK+accuracyK+1)=pi/maxX;
ky(accuracyK+2:accuracyK+accuracyK+1)=...
            pi/maxY/accuracyK:pi/maxY/accuracyK:pi/maxY;

kx(accuracyK+2+accuracyK:accuracyK+accuracyK+1+accuracyK)=...
        pi/maxX−pi/maxX/accuracyK:−pi/maxX/accuracyK:0;
ky(accuracyK+2+accuracyK:accuracyK+accuracyK+1+accuracyK)=...
        pi/maxY−pi/maxY/accuracyK:−pi/maxY/accuracyK:0;
```

```
%Crating the figure
figure;
ax1=axes;
hold on;

%Counter of the wave vector points
curr_vector=0;

%% The cycle for all the points in k−path
for phase=1:length(kx)
    curr_vector=curr_vector+1;
    %Computing phase shift for a specific wave vector
    rotatex=(exp(−1i*(kx(phase)*maxX)));
    rotatey=(exp(−1i*(ky(phase)*maxY)));

    %Cleaning the computation region
    Ez=zeros(accuracyX,accuracyY);
    Hx=zeros(accuracyX,accuracyY);
    Hy=zeros(accuracyX,accuracyY);

    %Ecxitation is defined as Delta−function in a single point
    Ez(round(accuracyX/3),round(accuracyY/4))=100;

    %% Cycle for time
    for t=0:Dt:maxT*Dt

        %% Computing H−field

        %Defining periodic boundary conditions for H−field

        for x=1:accuracyX
            Hx(x,1)=Hx(x,1)−c*Dt/mu/Dy*(Ez(x,1)−rotatey*...
                                    Ez(x,accuracyY));
        end
        for y=2:accuracyY
            Hx(1,y)=Hx(1,y)−c*Dt/mu/Dy*(Ez(1,y)−Ez(1,y−1));
        end

        for x=2:accuracyX
            Hy(x,1)=Hy(x,1)+c*Dt/mu/Dx*(Ez(x,1)−Ez(x−1,1));
        end
        for y=1:accuracyY
            Hy(1,y)=Hy(1,y)+c*Dt/mu/Dx*(Ez(1,y)−rotatex*...
                                    Ez(accuracyX,y));
        end
```

%% Computing the H–field distribution

```
for y=2:accuracyY
    for x=2:accuracyX
        Hx(x,y)=Hx(x,y)−c*Dt/mu/Dy*(Ez(x,y)−Ez(x,y−1));
        Hy(x,y)=Hy(x,y)+c*Dt/mu/Dx*(Ez(x,y)−Ez(x−1,y));
    end
end
```

%% Computing E–field

```
for y=1:accuracyY−1
    for x=1:accuracyX−1
        Ez(x,y)=Ez(x,y)+eps_x(x,y)*(Hy(x+1,y)−Hy(x,y))−...
                    eps_y(x,y)*(Hx(x,y+1)−Hx(x,y));
    end
end
```

%% Defining periodic boundary conditions for E

```
for x=1:accuracyX−1
    Ez(x,accuracyY)=Ez(x,accuracyY)+...
 eps_x(x,accuracyY)*(Hy(x+1,accuracyY)−Hy(x,accuracyY))−...
 eps_y(x,accuracyY)*(Hx(x,1)/rotatey−Hx(x,accuracyY));
end

for y=1:accuracyY−1
    Ez(accuracyX,y)=Ez(accuracyX,y)+...
 eps_x(accuracyX,y)*(Hy(1,y)/rotatex−Hy(accuracyX,y))−...
 eps_y(accuracyX,y)*(Hx(accuracyX,y+1)−Hx(accuracyX,y));
end
Ez(accuracyX,accuracyY)=Ez(accuracyX,accuracyY)+...
    eps_x(accuracyX,accuracyY)*...
    (Hy(1,accuracyY)/rotatex−Hy(accuracyX,accuracyY))−...
    eps_y(accuracyX,accuracyY)*...
    (Hx(accuracyX,1)/rotatey−Hx(accuracyX,accuracyY));

Eres(round(t/Dt)+1)=Ez(round(accuracyX/3),round(accuracyY/7));
Time(round(t/Dt)+1)=t;
```

end

%% Analyzing the temporal response
%Computing the Fourier transform of the response
fourier=abs(fft(Eres));

%Normalizing frequency

```
f=1/Dt*(0:length(fourier)−1)/length(Eres);

%eigen−frequencies counter
wcount=1;

%Analyzing the first point of the spectrum
if(fourier(1)/(max(fourier(2:4)))>1.1)
    weigen(curr_vector, wcount)=f(1);
    wcount=wcount+1;
end

%Analyzing the rest of the spectrum
for u=3:length(fourier)−3
    if(fourier(u)/(max(fourier(u+1:u+2)))>1.01)&&...
            (fourier(u)/max(fourier(u−2:u−1))>1.01)
        weigen(curr_vector, wcount)=f(u);
        wcount=wcount+1;
    end
end

%Plotting 5 solutions maximum
if(wcount−1>=5)
 plot(curr_vector,abs(weigen(curr_vector,1:5))*maxX/c,'ob');
else
 plot(curr_vector,abs(weigen(curr_vector,1:wcount−1))*maxX/c,'ob');

end
%Decoraring the plot
set(ax1,'xtick',[1 accuracyK+1 2*accuracyK+1 3*accuracyK+1]);
set(ax1,'xticklabel',['G';'X';'M';'G']);
ylabel('Frequency \omegaa/2\pic','FontSize',14);
xlabel('Wavevector','FontSize',14);
set(ax1,'XGrid','on');

drawnow;

end
```

The results computed by the presented code are given in figure 7 . The parameters in the program are selected to eliminate the spurious solutions. However, if an input power is changed, one should change the accuracy in the spectrum analysis part.

4.2. Bistable nonlinear PhCs

Nonlinear PhC filters with properly selected parameters, possess bistability and can be used as logical gates in all-optical data processing systems. In this section, we give an example of such filters on the basis of 2D PhC [5].
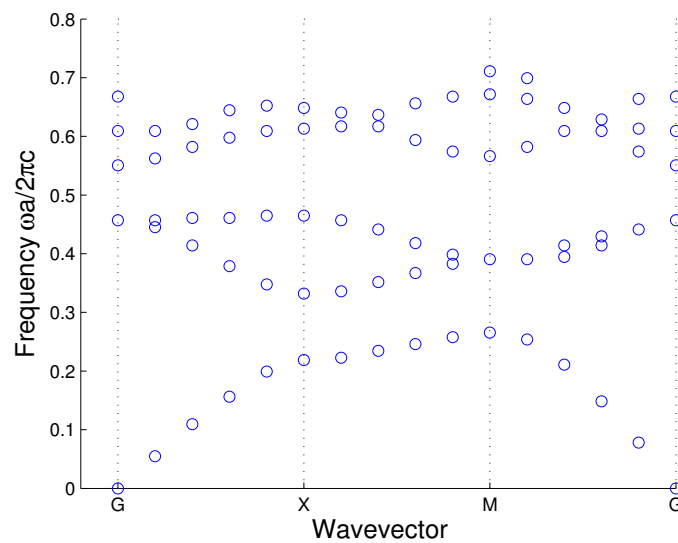
**Figure 7.** Band structure of 2D PhC computed by the FDTD method
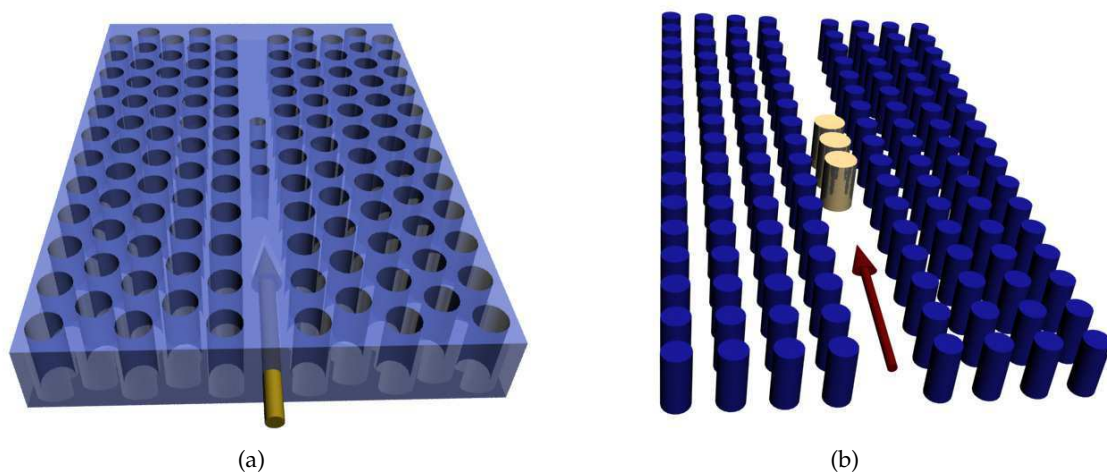
Figure 8. The structure of the investigated nonlinear PhC confined by the PhC waveguide on the basis of hexagonal (a) and square (b) lattice

The schematic of investigated nonlinear PhC filter confined by the PhC waveguide is shown in the figure 8.

In both cases, the PhC filter is presented by three PhC elements with parameters similar to the confined PhC. The photonic bandgap (PBG) of the filters are shifted as respect to the background PhC. As it has been demonstrated for the linear PhCs, such filters almost do not disturb an ultra-short pulses shape.

Initially, the operating wavelength $\lambda = 1.05~\mu m$ is selected to fall at the PBG of both background PhC and filter. However, due to optical nonlinearity the spectral characteristic of the filter appears to be shifted when increasing the radiation intensity.
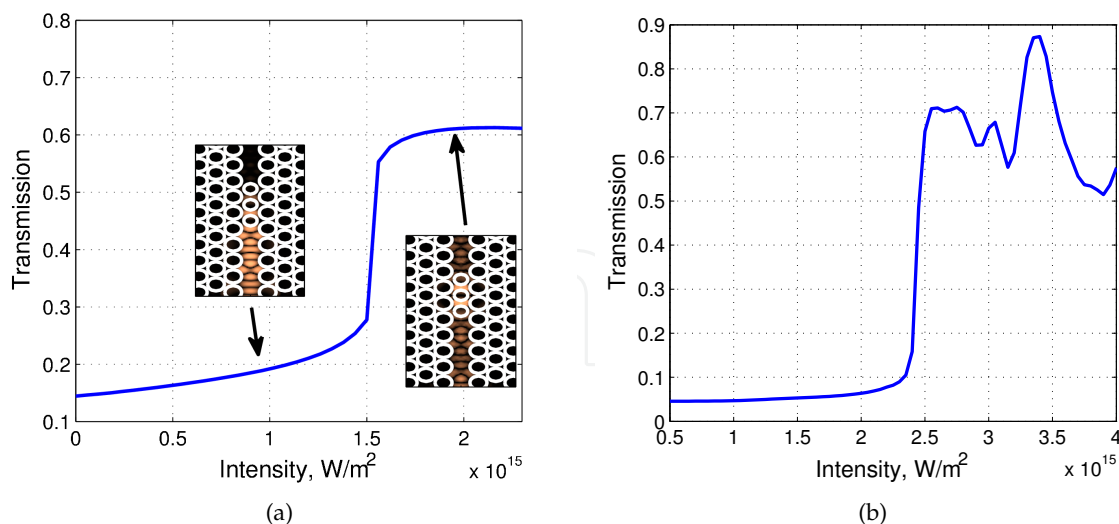
Figure 9. Transmission of the filter as a function of the input intensity in case of hexagonal PhC (a) and square PhC (b)

The reaction of the structure to increasing radiation intensity is presented in figure 9. The figure represents filter transmission as a function of the intensity of the CW monochromatic radiation. The insertions demonstrate the field behavior inside the waveguide with nonlinear PhC filter in case of low and high radiation intensity.

The results in the figure 9 allow to conclude that starting at certain value of the intensity, the radiation wavelength appears outside the PBG which increases transmission of such a filter dramatically. The further growth of the nonlinearity no longer increases the transmission as is seen from the figure 9. Therefore, in our investigation we have selected operating intensity slightly below the switching-on intensity.

Since the PhCs and, particularly, PhC-based filters possess resonant radiation transmission (the radiation is propagating from one element to another), the nonlinear spectrum shift require certain time which does not rely on response time of the nonlinear material. In order to investigate such a phenomena, we carried out the study of temporal response of such a filter to Gaussian pulses of different durations. Each of the pulses in serie possesses the same magnitude but different duration. The photorefractive properties of the materials remain the same for all pulses. This allows investigating only the contribution of the resonant processes inside the PhC into the bistability.

After the temporal response is obtained, it is represented in form of the dependence of output intensity on the input one as presented in figure 10. The intensity growth corresponds to the lowest branch of the hysteresis loop and lowering of the intensity stands for highest branch. Both in case of hexagonal and square lattices such characteristics look almost the same and, therefore, we provide here only the ones for the hexagonal PhC.

In case of linear optical materials, the branches are coincide since no processes affect the properties of the PhC. However, in case of nonlinear materials the light trapped inside the filter due to resonances holds the refractive index of the nonlinear material and, consequently, the transmission of the filter, high, thus, providing the difference in propagation of the leading and trailing edges of the pulse.
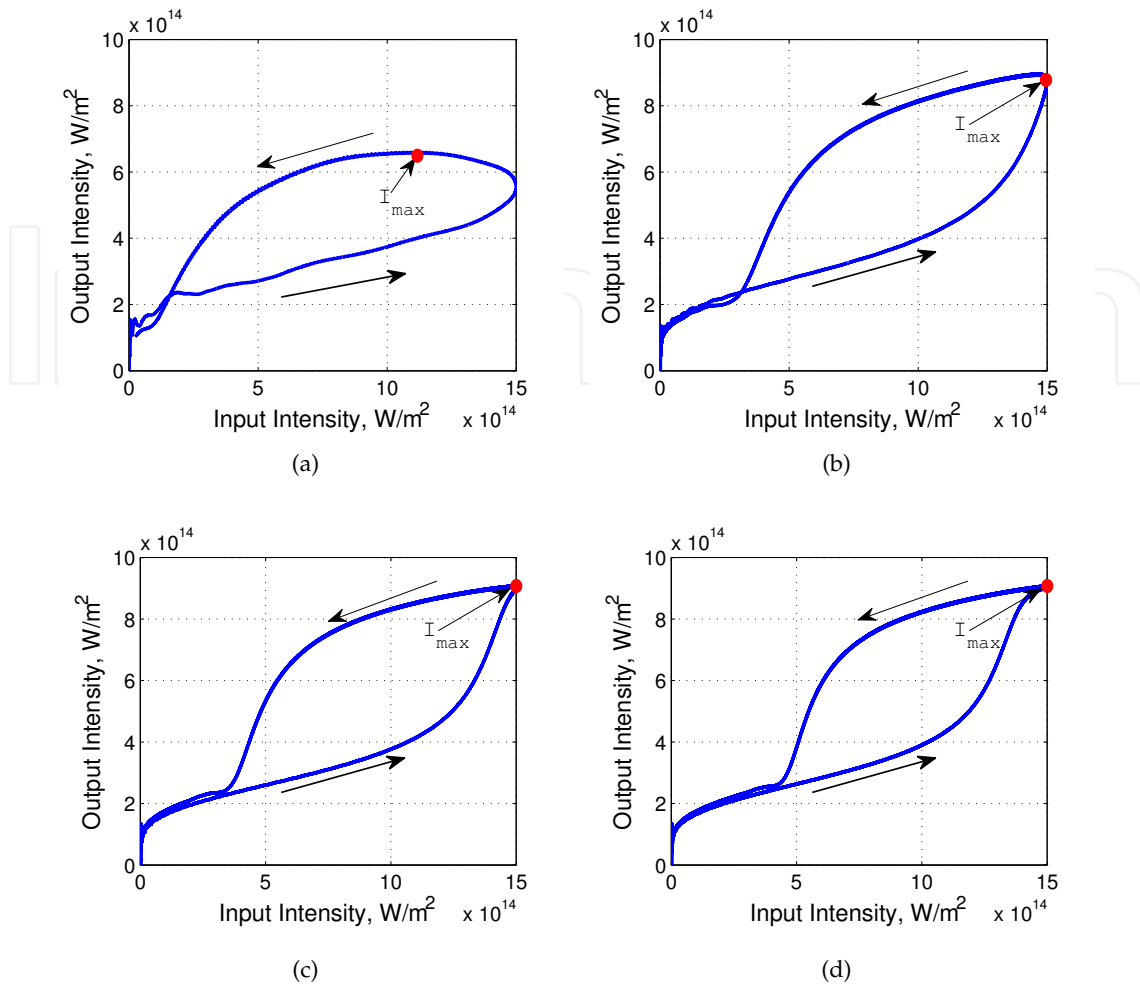
Figure 10. Hysteresis loops at different durations of the Gaussian pulse: a) $\tau = 50\ fs$, b) $\tau = 200\ fs$, c) $\tau = 400\ fs$, d) $\tau = 800\ fs$

Due to finite saturation time of the resonances in the PhC, the minimum allowed pulse duration exists for a specific PhC filter. Normally, during the front edge of Gaussian pulse, the intensity inside the filter grows which causes refractive index changes and, consequently, the changes in the filter characteristic. However, if the pulse duration is lower than the time required to excite the eigen-state in the filter, the significant nonlinear effects such as transmission growth appear after the input pulse maximum (see figure 10(a)). On the other hand, when the pulse duration is large, it is enough to excite the filter and, therefore, the maximum intensity of the input and output pulses are coincide.

Thus, the study of the temporal responses carried out in the work demonstrates the possibility of all-optical switching of the filter by the pulses which increase of reduce the intensity temporarily and, consequently, change the filter state.

After this we have studied its nonlinear switching dynamics. For this reason the continuous wave pump signal is launched into the waveguide. Then, with certain delays, the Gaussian control signals are launched which turn on and turn off the transmission of the filter. The power of the pump signal corresponds to the maximum magnitude of the hysteresis loop.
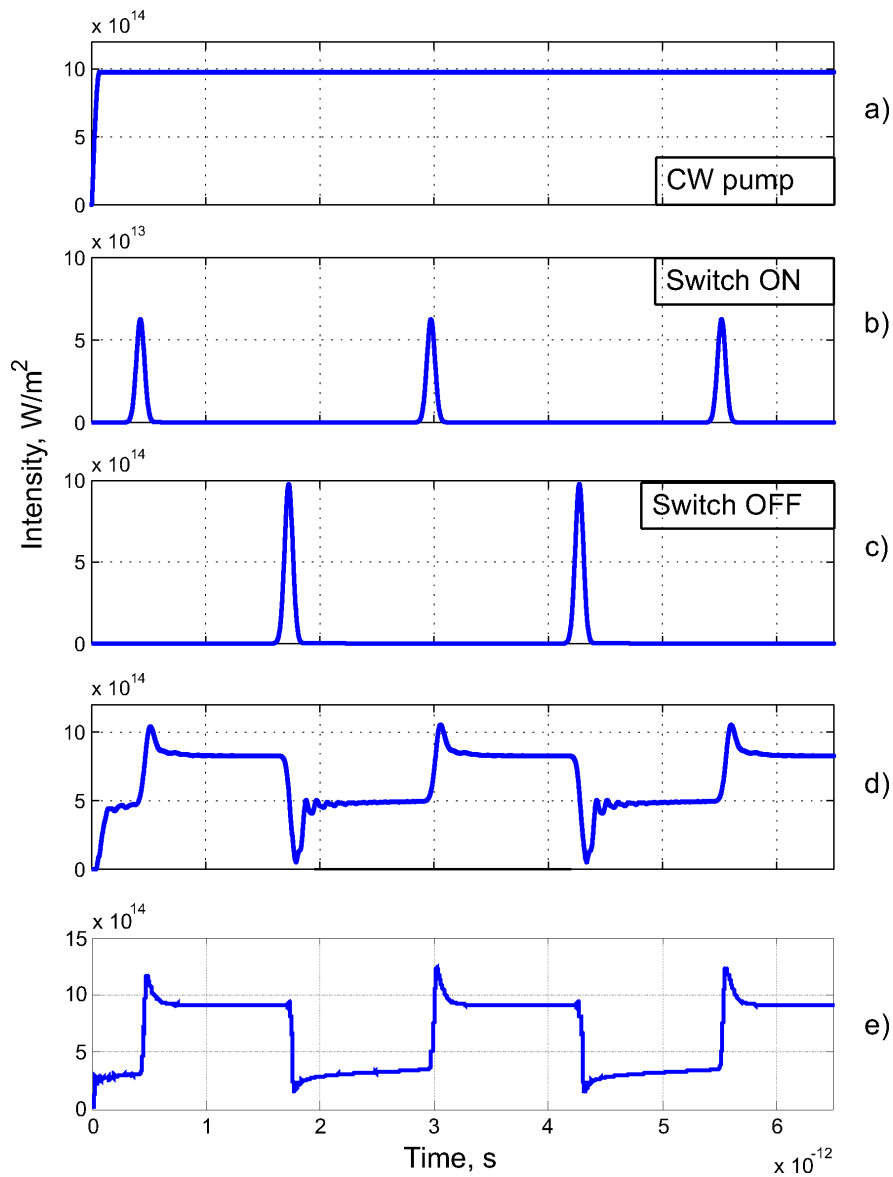
Figure 11. The CW pump (a), ON (b), OFF (c) and resulting signal in hexagonal (d) and square (e) PhC

Switching ON occurs when the Gaussian signal is launched with the same phase as the pump one. If the signal possesses opposite phase, switching OFF occurs.

The temporal response of the investigated filter is demonstrated in the figure 11. The topmost figure shows the intensity of the pump signal. The figures 11(b) and 11(c) demonstrate turn on and turn off pulses sequences. In two lowest figures, the resulting output signals are shown in case of hexagonal and square PhC lattices.

The pump signal intensity is slightly below the nonlinearity threshold. Therefore, switching ON requires low intensity Gaussian pulse. On the other hand, when switching OFF, the signal intensity should be reduced down to $2 \cdot 10^{14} \ W/m^2$ as follows from the figure 10(d). Therefore, the switching OFF signal maximum intensity is taken the same as that of the pump signal.

Comparing two nonlinear wideband filters we can mention their efficiency as bistable devices. However, at the same conditions transition time is larger in case of hexagonal PhC. On the other hand, in square PhC the lower radiation level is not as stable as the higher one and the output intensity in this case grows raising the probability of bit error.

Nevertheless, both these filters can be used as a basic logic in all-optical data processing circuits and the choice will be determined only by the technological factors.

4.3. Conclusions

In the chapter, we have demonstrated several applications of temporal characteristics as well as their computation method for both linear and nonlinear PhC wideband filters. Such micro-devices as wideband filters, wavelength division multiplexers and bistable elements may become a basis for future all-optical integrated circuits.

Presented Matlab codes for building an eye-diagram and for computing the band structure of 2D PhC by means of the FDTD methods will be useful for master and PhD students working on design and optimization of PhC-based micro-devices.

Author details

I. V. Guryev⋆, J. R. Cabrera Esteves,
I. A. Sukhoivanov, N. S. Gurieva, J. A. Andrade Lucio,
O. Ibarra-Manzano and E. Vargas Rodriguez

⋆ Address all correspondence to: guryev@ieee.org

University of Guanajuato, Campus Irapuato-Salamanca, Division of Engineering, Mexico

References

[1] Berenger, J. [1994]. A perfectly matched layer for the absorption of electromagnetic waves, *Journal of Computational Physics* 114: 185–200.

[2] Bian, S., Martinelli, M. & Horowicz, R. J. [1999]. Z-scan formula for saturable kerr media, *Opt. Commun.* 172: 347–353.

[3] Brenner, N. & Rader, C. [1976]. A new principle for fast fourier transformation, *IEEE Trans. Acoust. Speech Signal Process* 24: 264–266.

[4] Greene, J. H. & Taflove, A. [2006]. General vector auxiliary differential equation finite-difference time-domain method for nonlinear optics, *Opt. Express* 14(18): 8305–8310.

[5] Guryev, I., Sukhoivanov, I., Lucio, J. A. & Rodriguez, E. V. [2012]. All-optical flip-flop in wideband phc-based flter with kerr saturable nonlinearity, *Applied Physics B* 106(3): 645–651.

[6] Guryev, I. V., Sukhoivanov, I. A., Lucio, J. A. A., Manzano, O. G. I. & Rodriguez, E. V. [2012]. Comprehensive analysys of the phcbased filters for optical micro-devices engineering, *Optical Engineering* 51(7): 074002.

[7] Joannopoulos, J., Meade, R. & Winn, J. [1995]. *Photonic Crystals: Molding the Flow of Light*, Princeton University Press, Princeton.

[8] Sukhoivanov, I. & Guryev, I. [2009]. *Photonic crystals – physics and practical modeling*, Optical sciences, 1 edn, Springer, Berlin.

[9] Sukhoivanov, I., Guryev, I., Andrade-Lucio, J., Alvarado-Méndez, E., Trejo-Durán, M. & Torres-Cisneros, M. [2008]. Photonic density of states maps for design of photonic crystal devices, *Microelectronics Journal* 39: 685–689.

[10] Sukumar, N. & Pask, J. E. [2009]. Classical and enriched finite element formulations for bloch-periodic boundary conditions, *International Journal for Numerical Methods in Engineering* 77(8): 1121–1138.

[11] Taflove, A. & Hagness, S. [2005]. *Computational Electrodynamics: The Finite-Difference Time-Domain Method*, 3 edn, Artech House, Norwood, MA.

[12] Yu, H. & Yang, D. [1996]. Finite difference analysis of 2-d photonic crystals, *IEEE Transaction On Microwave Theory And Techniques* 44(12): 2688–2695.